

Diradical and Peroxirane Pathways in the $[\pi 2 + \pi 2]$ Cycloaddition Reactions of $^1\Delta_g$ Dioxygen with Ethene, Methyl Vinyl Ether, and Butadiene: A Density Functional and Multireference Perturbation Theory Study

Andrea Maranzana, Giovanni Ghigo, and Glauco Tonachini*[†]

Contribution from the Dipartimento di Chimica Generale e Organica Applicata, Università di Torino, Corso Massimo D'Azeglio 48, 10125 Torino, Italy

Received March 12, 1999. Revised Manuscript Received November 24, 1999

Abstract: The main purpose of this study is to assess the relative importance of diradical or peroxirane (perepoxide) intermediates in the singlet oxygen cycloaddition reactions with alkenes that lead to dioxetanes. The relevant nonconcerted pathways are explored for ethene, methyl vinyl ether, and *s-trans*-butadiene by CAS-MCSCF optimizations followed by multireference perturbative CAS-PT2 energy calculations and by DFT(B3LYP) optimizations. The two different theoretical approaches gave similar results (reported below). These results show that methoxy or vinyl substitution does not affect qualitatively the reaction features evidenced by the unsubstituted system. Peroxirane turns out to be attainable only by passing through the diradical, due to the nature of the critical points involved. The energy barriers for the transformation of the diradical to peroxirane in the case of ethene ($\Delta E^\ddagger = 13\text{--}15$ kcal mol⁻¹) and methyl vinyl ether ($\Delta E^\ddagger = 12\text{--}13$ kcal mol⁻¹) are higher than those for the diradical closure to dioxetane ($\Delta E^\ddagger = 8\text{--}9$ kcal mol⁻¹, for ethene, and 9 kcal mol⁻¹, for methyl vinyl ether). In all three systems, the peroxirane pathway to dioxetane is prevented by the high energy barrier for the second step, leading from peroxirane to dioxetane ($\Delta E^\ddagger = 26\text{--}27$, $27\text{--}31$ and 22 kcal mol⁻¹, for ethene, methyl vinyl ether, and butadiene, respectively). By contrast, peroxirane can very easily back-transform to the diradical (with a ΔE^\ddagger estimate of 3 kcal mol⁻¹, for ethene and methyl vinyl ether, and close to zero, for butadiene). These results indicate that, although a peroxirane intermediate might form in some cases, it corresponds to a dead-end pathway which cannot lead to dioxetane.

Introduction

$^1\Delta_g$ dioxygen, the first (degenerate) excited state of O₂, is quite an important reactive species in oxidation reactions.^{1,2a} The literature dealing with occurrence, preparation, reactions, and reaction mechanisms of this ubiquitous molecule is vast, and here only some of these aspects will be briefly mentioned. Beside its preparation by photochemical or chemical means,^{2a} $^1\Delta_g$ O₂ is produced by ozone photolysis in the troposphere^{2b,3} or in the oxidation and combustion of hydrocarbons (autoxidation).^{2c,4a} It can be generated also by action of metal catalysts on H₂O₂.^{2d,5a} Its reactions range from processes exploited for synthetic purposes,^{2a} to the (dangerous) intervention in biochemical events, e.g. the attack to the DNA base guanine.^{5b} Indeed, singlet oxygen is known to damage also organic tissues, and its reactions with some biomolecules have been investigated.^{2e}

[†] E-mail: tonachini@ch.unito.it.

(1) Gilbert, A.; Baggott, J. *Essentials of Molecular Photochemistry*; Blackwell Science: Cambridge, MA, 1995; Chapter 11.

(2) (a) Foote, C. S.; Clennan, E. L. *Properties and Reactions of Singlet Dioxygen*. In *Active Oxygen in Chemistry*; Foote, C. S., Valentine, J. S., Greenberg, A., Liebman, J. F., Eds.; Blackie Academic and Professional (Chapmann & Hall): New York, 1995; Chapter 4. (b) Atkinson, R. *Reactions of Oxygen Species in the Atmosphere*. *Ibid.*, Chapter 7. (c) Dussault, P. *Reactions of Hydroperoxides and Peroxides*. *Ibid.*, Chapter 5, pp 176, 177. (d) Bielski, B. H.; Cabelli, D. E. *Superoxide and Hydroxyl Radical Chemistry in Aqueous Solution*. *Ibid.*, Chapter 7. (e) See ref 2a, pp 107–109, 119, 120, and 132, for some recent studies.

(3) Wayne, R. P. *Chemistry of Atmospheres*; Clarendon Press: Oxford, U.K., 1996; p 86.

Singlet dioxygen reacts with organic unsaturated substrates with the main four addition modes shown in Scheme 1.^{6–8}

The $[\pi 2 + \pi 2]$ addition to one double CC bond results in 1,2-dioxetane. The $[\pi 4 + \pi 2]$ addition to a conjugated diene produces an endoperoxide. If one allylic hydrogen is available, the outcome can be the formation of a hydroperoxide (ene

(4) Plesnicar, B. *Polyoxides*. In *Organic Peroxides*; Ando, W., Ed.; John Wiley and Sons: New York, 1992; Chapter 10, pp 489–494. (b) Yamaguchi, K.; Takada, K.; Otsuji, Y.; Mizuno, K. *Theoretical and General Aspects of Organic Peroxides*. *Ibid.*, Chapter 1, pp 65–68. (c) The other one is the Kopecky method, a β -halo hydroperoxide cyclization. See: Adam, W.; Heil, M.; Mosland, T.; Saha-Möller, C. R. *Dioxetanes and α -Peroxylactones, Ring Cyclic Peroxides*. *Ibid.*, Chapter 5, p 223 ff. For other synthetic methods, see for instance: Lopez, L.; Farinola, G. M.; Nacci, A.; Sportelli, S. *Tetrahedron* **1998**, *54*, 6939–6946. Lopez, L.; Troisi L. *Tetrahedron* **1992**, *48*, 7321–7330. Lopez, L.; Troisi, L. *Gazz. Chim. Ital.* **1992**, *122*, 507–509. Lopez, L.; Troisi, L.; Mele, G. *Tetrahedron Lett.* **1991**, *32*, 117–120. Posner, G. H.; Webb, K. S.; Nelson, W. M.; Kishimoto, T.; Seliger, H. H. *J. Org. Chem.* **1989**, *54*, 3252–3254. Curci, R.; Lopez, L.; Troisi, L.; Rashid, S. M. K.; Schaap, A. P. *Tetrahedron Lett.* **1988**, *29*, 3145–3148. Curci, R.; Lopez, L.; Troisi, L.; Rashid, S. M. K.; Schaap, A. P. *Tetrahedron Lett.* **1987**, *28*, 5319–5322. (d) Reference 4c, p 221.

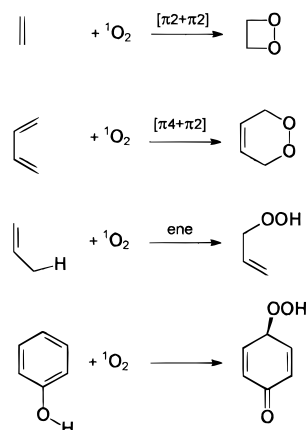
(5) (a) Marusak, R. A.; Meares, C. F. *Metal-Complex Catalyzed Cleavage of Biopolymers*. In *Active Oxygen in Biochemistry*; Valentine, J. S., Foote, C. S., Greenberg, A., Liebman, J. F., Eds.; Blackie Academic and Professional (Chapmann & Hall): New York, 1995; Chapter 8. (b) Halliwell, B. *The Biological Significance of Oxygen-Derived Species*. *Ibid.*, Chapter 7. (c) Greenberg, A. *Exploration of Selected Pathways for Metabolic Oxidative Ring Opening of Benzene Based on Estimates of Molecular Energetics*. *Ibid.*, Chapter 9, pp 415–419.

(6) March, J. *Advanced Organic Chemistry*, 4th ed.; J. Wiley & Sons: New York, 1992; Chapter 5, Section 37.

(7) Jefford, C. W. *Chem. Soc. Rev.* **1993**, 59–66.

(8) Frimer, A. A. *Chem. Rev.* **1979**, *79*, 359–387.

Scheme 1



reaction, structurally related to the preceding one). These three reactions can compete on the same substrate, if the molecular structure allows it.⁹ With electron-rich alkenes dioxetane formation prevails over hydroperoxide formation. Finally, singlet dioxygen is known to add to phenol derivatives, in a reaction which is similar to the ene mode and yields hydroperoxide ketones.¹⁰

The $[\pi 2 + \pi 2]$ addition investigated in this paper is one of the two rather general methods for 1,2-dioxetane synthesis.^{4c} Actual dioxetane formation is detected when structural features (such as the presence of bulky substituents) impede its decomposition into two carbonyl moieties, which are otherwise the final result of this reaction.^{7,11,12} Stable dioxetanes of this kind, whose chemiluminescent fragmentation can be activated enzymatically, have been found useful in biomedical applications.^{12d,e} It can also be incidentally recalled that dioxetane intervention in biochemical oxidation of benzene through a $[\pi 2 + \pi 2]$ addition was proposed in several instances,⁸ but this kind of hypothesis has been recently discarded on the basis of thermochemical arguments.^{5c} In fact, singlet oxygen has been reported to react with electron-rich benzenes and polycyclic aromatic hydrocarbons yielding endoperoxides via a $[\pi 4 + \pi 2]$ cycloaddition.^{2a}

A large number of experimental studies have been devoted to the elucidation of the mechanisms of cycloaddition of $^1\Delta_g$ O₂ to carbon-carbon multiple bonds. In particular, the question of a concerted versus nonconcerted mechanism has been addressed for all modes of pericyclic reactivity.¹³ Although a large amount of disparate evidence has been collected, no ultimate answers appear to be available at the moment. For instance, the Diels-Alder-like endoperoxide formation has been

(9) See for instance: (a) Clennan, E. L. *Tetrahedron* **1991**, *47*, 1343–1382 (Tetrahedron Report No. 285). (b) Vassilikogiannakis, G.; Stratakis, M.; Orfanopoulos, M. *J. Org. Chem.* **1998**, *63*, 6390–6393. (c) Griesbeck, A. G.; Fiege, M.; Gudipati, M. S.; Wagner, R. *Eur. J. Org. Chem.* **1998**, 2833–2838.

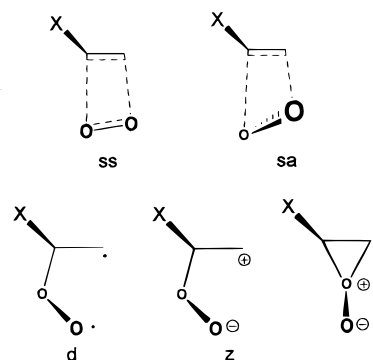
(10) Lissi, E. A.; Encinas, M. V.; Lemp, E.; Rubio, M. A. *Chem. Rev.* **1993**, *93*, 699–723.

(11) Adam, W.; Saha-Möller, C. R.; Schambony, S. B. *J. Am. Chem. Soc.* **1999**, *121*, 1834–1838.

(12) (a) Schaap, A. P.; Faler, G. R. *J. Am. Chem. Soc.* **1973**, *95*, 3381–3382. (b) Zaklika, K. A.; Kaskar, B.; Schaap, A. P. *J. Am. Chem. Soc.* **1980**, *102*, 386–389. (c) Schaap, A. P.; Recher, S. G.; Faler, G. R.; Villasenor, S. R. *J. Am. Chem. Soc.* **1983**, *105*, 1691–1693. (d) Akhavan-Tafti, H.; Eickholt, R. A.; Arghavani, Z.; Schaap, A. P. *J. Am. Chem. Soc.* **1997**, *119*, 245–246. (e) Schaap, A. P.; Handley, R. S.; Giri, B. P. *Tetrahedron Lett.* **1987**, *28*, 935–938. (f) Schaap, A. P.; Zaklika, K. A. 1,2 Cycloadditions Reactions of Singlet Oxygen. In *Singlet Oxygen, a Monograph in the Organic Chemistry Series*; Wasserman, H. H., Murray, R. W., Eds.; Academic Press: New York, 1979; Chapter 6.

(13) Prein, M.; Adam, W. *Angew. Chem., Int. Ed. Engl.* **1996**, *35*, 477–494 and refs 7–23 therein.

Scheme 2



generally considered a concerted reaction, but kinetic evidence was in some cases in favor of a two-step mechanism.¹⁴ Even the mechanism of the apparently elementary $[\pi 2 + \pi 2]$ reaction, which forms the subject of the present study, cannot be yet considered as assessed. Divergent reaction mechanisms have been proposed in the past,^{7,8} on the basis of the experimental evidence collected on different molecular systems. These pathways range from concerted approaches as supra-supra or supra-antara (ss, sa in Scheme 2), to nonconcerted ones, which can see the intervention of diradical, open-chain zwitterionic or peroxidic (peroxirane) intermediates (d, z, and p, respectively, in Scheme 2).

Some researchers have postulated the intervention of more or less loosely structured exciplexes, not only for the $[\pi 2 + \pi 2]$ but also for the $[\pi 4 + \pi 2]$ and ene additions.^{15,16} Evidence for nonconcerted pathways in the ene and $[\pi 2 + \pi 2]$ reactions has been collected.^{16,20c} Stereochemical studies,^{11,13,16–19} as well as kinetic isotope effect experiments concerning the ene reaction,^{9,20} have yielded results which are seemingly best explained by postulating a peroxirane intermediate or a peroxirane-like exciplex.²¹ These two reactions, which often compete for the same substrate,²² might share the intermediacy of the same zwitterionic (either peroxidic or open-chain) or diradical

(14) (a) Clennan, E. L.; Mersheikh-Mohammadi, M. E. *J. Am. Chem. Soc.* **1984**, *106*, 7112–7118. (b) Clennan, E. L.; Mersheikh-Mohammadi, M. E. *J. Org. Chem.* **1984**, *49*, 1321–1322.

(15) Aubry, J.-M.; Mandard-Cazin, B.; Rougee, M.; Bensasson, R. V. *J. Am. Chem. Soc.* **1995**, *117*, 9159–9164. (b) Kanner, R. C.; Foote, C. S. *J. Am. Chem. Soc.* **1992**, *114*, 682–688. (c) Gorman, A. A.; Gould, I. R.; Hamblett, I. *J. Am. Chem. Soc.* **1982**, *104*, 7098–7104.

(16) Adam, W.; Prein, M. *Acc. Chem. Res.* **1996**, *29*, 275–283.

(17) Brünker, H.-G.; Adam, W. *J. Am. Chem. Soc.* **1995**, *117*, 3976–3982.

(18) (a) Linker, T.; Rebien, F.; Tóth, G. *Chem. Commun.* **1996**, 2585–2586. (b) Frimer, A. A.; Bartlett, P. D.; Boschung, A. F.; Jewett, J. G. *J. Am. Chem. Soc.* **1977**, *99*, 7977–7986.

(19) (a) Orfanopoulos, M.; Grdina, M. B.; Stephenson, L. M. *J. Am. Chem. Soc.* **1979**, *101*, 275–276. (b) Schulte-Elte, K. H.; Rautenstrauch, V. *J. Am. Chem. Soc.* **1980**, *102*, 1738–1740. (c) Adam, W.; Catalani, L. H.; Griesbeck, A. *J. Org. Chem.* **1986**, *51*, 5494–5496. (d) Adam, W.; Prein, M. *J. Am. Chem. Soc.* **1993**, *115*, 3766–3767. (e) Stratakis, M.; Orfanopoulos, M.; Foote, C. S. *J. Org. Chem.* **1998**, *63*, 1315–1318.

(20) (a) Stephenson, L. M.; McClure, D. E.; Sysak, P. K. *J. Am. Chem. Soc.* **1973**, *95*, 7888–7889. (b) Grdina, M. B.; Orfanopoulos, M.; Stephenson, L. M. *J. Am. Chem. Soc.* **1979**, *101*, 3111–3112. (c) Orfanopoulos, M.; Smonou, I.; Foote, C. S. *J. Am. Chem. Soc.* **1990**, *112*, 3607–3614. (d) Stratakis, M.; Orfanopoulos, M.; Chen, J. S.; Foote, C. S. *Tetrahedron Lett.* **1996**, *37*, 4105–4108.

(21) (a) Poon, T. H. W.; Pringle, K.; Foote, C. S. *J. Am. Chem. Soc.* **1995**, *117*, 7611–7618. (b) Clennan, E. L.; Lewis, K. K. *J. Am. Chem. Soc.* **1987**, *109*, 2475–2478. (c) Stratakis, M.; Orfanopoulos, M. *Tetrahedron Lett.* **1995**, *36*, 4291–4294.

(22) (a) Matsumoto, M.; Kobayashi, H.; Matsubara, J.; Watanabe, N.; Yamashita, S.; Oguma, D.; Kitano, Y. M.; Ikawa, H. *Tetrahedron Lett.* **1996**, *37*, 397–400. (b) Matsumoto, M.; Kitano, Y.; Kobayashi, H.; Ikawa, H. *Tetrahedron Lett.* **1996**, *37*, 8191–8194. (c) Adam, W.; Kumar, A. S.; Saha-Möller, C. R. *Tetrahedron Lett.* **1995**, *43*, 7853–7854.

species.^{7,18} However, evidence for the intervention of a peroxirane in $[\pi 2 + \pi 2]$ cycloadditions is somewhat less compelling.^{12,23} The pathway for the ene seems however to be less polar than that for dioxetane formation.^{18b,20c}

Other researchers carried out theoretical investigations with the aim of elucidating the ene and $[\pi 2 + \pi 2]$ reaction mechanisms. Earlier studies,^{24,25} carried out at a semiempirical level of theory, pointed out that peroxide could play an important role. However, these studies indicated an open-chain zwitterion as the probable intermediate for alkenes with electron-donating substituents. By contrast, GVB-CI studies carried out a few years later were in favor of a diradical mechanism and located peroxirane at a higher energy than the diradical.²⁶ Further *ab initio* and semiempirical UHF calculations lead to the same description.²⁷ Yet, the computationally predicted and experimentally observed stereospecificity and regioselectivity led the authors to discard the diradicals as possible intermediates in the ene reactions and to suggest a concerted mechanism. A high-level CAS-MCSCF and CCI study (carried out however with symmetry-constrained geometry optimizations) defined the C_s peroxirane pathway as easier than a C_s (syn) diradical pathway.²⁸ That study did not provide information on lower-symmetry pathways, and the symmetry constraints did not allow the authors to specify if the nature of the C_s critical points so defined was that of genuine transition structures. Some more recent studies on ethene²⁹ and ethenol,³⁰ based on fully unrestricted geometry optimizations at the CAS-MCSCF theory level, provided some indication in favor of the direct formation of a diradical intermediate. While a peroxirane was also present as a further intermediate, it could only form by passing first through the open-chain intermediate. A recent paper³¹ has summarized the results obtained by the authors on the oxidation mechanism of alkenes, enol ethers, and enamines. The main conclusion, also based on the comparison with experimental results of a different nature, is that distinct mechanisms operate depending on the symmetry of the substrate and the electron-donating capabilities of the substituents.

This paper aims to contribute to the understanding of the relative importance of nonconcerted pathways to dioxetanes in the reactions of three simple alkene systems with singlet dioxygen: ethene itself (reaction a), methyl vinyl ether (mve, reaction b), and the *s-trans* isomer of butadiene (reaction c).

The last two are rather electron-rich alkenes, whose structure prevents the ene reaction. Vinyl ethers^{15c} and alkyl- or alkoxy-substituted "butadienes"^{21b,23} are experimentally known to undergo the $[\pi 2 + \pi 2]$ reaction. In some cases, when competition with other reactions is possible, dioxetane formation can be the preferential pathway (enhanced by an increase in solvent polarity)^{9a,18b,23a} or even the only one.^{22a}

Concerted pathways are not dealt with here in detail, as they have been characterized as higher-order saddle points of no direct chemical importance, confirming earlier results on ethene.^{29,32} As regards nonconcerted pathways, the distinction between a diradical and a zwitterion is rather rigid, because a carbon-oxygen diradical has some zwitterionic character,³³⁻³⁵ which can be thought of as possibly enhanceable by appropriate solvation effects. The intermediates encountered in this study are of this kind. Though the gas-phase calculations of this study have shown that situations of sharper zwitterionic character are pertinent to excited electronic states of the same molecules, polar diradicals can be considered as representative of pathways involving open-chain intermediates. The diradical pathway, so intended, will be one subject of the present investigation. Its antagonist will be the conceivable pathway leading to peroxirane. As mentioned above, it has often been maintained that peroxiranes intervene as intermediates in $[\pi 2 + \pi 2]$ singlet oxygen cycloadditions.^{6-9,12,19,20} The possible intervention and competition of diradical and peroxirane intermediates, as well as their interconversion, is the main subject of this investigation. A second goal is the assessment of the barrier heights for their transformation into dioxetanes.

Method

The study of the two model reactions was performed by determining the critical points and the related energy differences on the reaction energy hypersurfaces. Two different theoretical methods (A and B; see the following) were used to do this.

(A) The geometrical structures were fully optimized by gradient methods³⁶ at the CAS-MCSCF³⁷ level, with the polarized split-valence shell 6-31G(d) basis set.^{38a} To refine the energy difference estimates, dynamic correlation effects were then taken care of through multireference second-order perturbation theory calculations, at the CAS-PT2 level of theory.³⁹ The active space chosen for the geometry optimization of the separate reactants includes (i) the π system of the alkene (two orbitals for ethene and mve, four orbitals for butadiene) and (ii) the

(23) (a) Clennan, E. L.; Nagraba, K. *J. Am. Chem. Soc.* **1988**, *110*, 4312-4318. (b) Clennan, E. L.; L'Esperance, R. P. *J. Am. Chem. Soc.* **1985**, *107*, 5178-5182. (c) Clennan, E. L.; L'Esperance, R. P. *J. Org. Chem.* **1985**, *50*, 5424-5426. (d) O'Shea, K. E.; Foote, C. S. *J. Am. Chem. Soc.* **1988**, *110*, 7167-7170.

(24) (a) Inagaki, S.; Yamabe, S.; Fujimoto, H.; Fukui, K. *Bull. Chem. Soc. Jpn.* **1972**, *45*, 3510-3514. (b) Inagaki, S.; Fukui, K. *J. Am. Chem. Soc.* **1973**, *97*, 7480-7484.

(25) (a) Dewar, M. J. S. *Chem. Br.* **1975**, *11*, 97-106. (b) Dewar, M. J. S.; Thiel, W. *J. Am. Chem. Soc.* **1975**, *97*, 3978-3986. (c) Dewar, M. J. S.; Griffin, A. C.; Thiel, W.; Turchi, I. J. *J. Am. Chem. Soc.* **1975**, *97*, 4439-4440.

(26) (a) Harding, L. B.; Goddard, W. A., III. *J. Am. Chem. Soc.* **1977**, *99*, 4520-4523. (b) Harding, L. B.; Goddard, W. A., III. *Tetrahedron Lett.* **1978**, *8*, 747-750. (c) Harding, L. B.; Goddard, W. A., III. *J. Am. Chem. Soc.* **1980**, *102*, 439-449.

(27) Yamaguchi, K.; Yabushita, S.; Fueno, T.; Houk, K. N. *J. Am. Chem. Soc.* **1981**, *103*, 5043-5046.

(28) Hotokka, M.; Roos, B.; Siegbahn, P. J. *J. Am. Chem. Soc.* **1983**, *105*, 5263-5269.

(29) (a) Tonachini, G.; Schlegel, H. B.; Bernardi, F.; Robb, M. A. *Theochem* **1986**, *138*, 221-227. (b) Tonachini, G.; Schlegel, H. B.; Bernardi, F.; Robb, M. A. *J. Am. Chem. Soc.* **1990**, *112*, 483-491.

(30) Liwo, A.; Dyl, D.; Jeziorek, D.; Novaka, M.; Ossowski, T.; Woznicki, W. *J. Comput. Chem.* **1997**, *18*, 1668-1681.

(31) Yoshioka, Y.; Yamada, S.; Kawakami, T.; Nishino, M.; Yamaguchi, K.; Saito, I. *Bull. Chem. Soc. Jpn.* **1996**, *69*, 2683-2699 and references therein.

(32) Maranzana, A. Tesi di Laurea, Università di Torino, II Facoltà di Scienze, Sede di Alessandria, Dec **1997**.

(33) Salem, L.; Rowland, C. *Angew. Chem., Int. Ed. Eng.* **1972**, *11*, 92-111.

(34) (a) Jug, K.; Poredda, A. *Chem. Phys. Lett.* **1990**, *171*, 394-399. (b) Jug, K.; Kölle, C. *J. Phys. Chem. B* **1998**, *102*, 6605-6611. (c) Jug, K. *Tetrahedron Lett.* **1985**, *26*, 1437-1440.


(35) (a) Michl, J.; Bonačić-Koutecký, V. *Electronic Aspects of Organic Photochemistry*; J. Wiley & Sons: New York, 1990; Chapter 4, Section 4. (b) Michl, J.; Bonačić-Koutecký, V. *Tetrahedron* **1988**, *44*, 7559-7585. (c) Bonačić-Koutecký, V.; Koutecký, J.; Michl, J. *Angew. Chem., Int. Ed. Engl.* **1987**, *26*, 170-189.

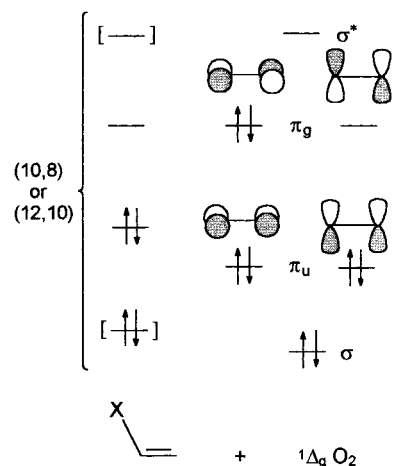
(36) Schlegel, H. B. In *Computational Theoretical Organic Chemistry*; Csizmadia, I. G., Daudel, R., Eds.; D. Reidel Publ. Co.: Dordrecht, The Netherlands, 1981; pp 129-159. Schlegel, H. B. *J. Chem. Phys.* **1982**, *77*, 3676-3681. Schlegel, H. B.; Binkley, J. S.; Pople, J. A. *J. Chem. Phys.* **1984**, *80*, 1976-1981. Schlegel, H. B. *J. Comput. Chem.* **1982**, *3*, 214-218.

(37) Robb, M. A.; Eade, R. H. A. *NATO Adv. Study Inst. Ser.* **1981**, *C67*, 21. See also, for a discussion of the method: Roos, B. The Complete Active Space Self-Consistent Field Method and its Applications in Electronic Structure Calculations. In: *Ab Initio Methods in Quantum Chemistry-II*; Lawley, K. P., Ed.; J. Wiley & Sons Ltd.: New York, 1987.

(38) (a) Hehre, W. J.; Ditchfield, R.; Pople, J. A. *J. Chem. Phys.* **1972**, *56*, 2257-2261. Hariharan, P. C.; Pople, J. A. *Theor. Chim. Acta* **1973**, *28*, 213-222. (b) Clark, T.; Chandrasekhar, J.; Schleyer, P. v. R. *J. Comput. Chem.* **1983**, *4*, 294-301. Frisch, M. J.; Pople, J. A.; Binkley, J. S. *J. Chem. Phys.* **1984**, *80*, 3265-3269.

Scheme 3

Out-of-phase counterparts () of the lone pair orbitals: when introduced in the final single-point energy calculations, they provide a (10,10) or (12,12) active space



two π_u , the two π_g , and the σ_{OO} , σ^*_{OO} orbitals of O_2 . This choice is shown in Scheme 3, where X = H, OMe, and vinyl. The two additional π levels introduced in the last case are drawn between brackets.

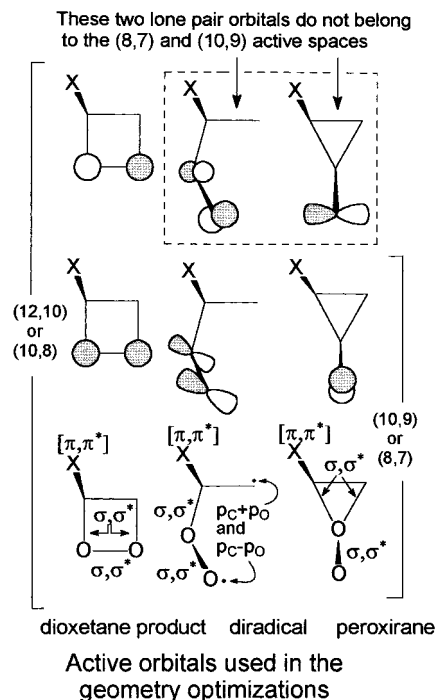
This set of 8 or 10 orbitals is populated by 10 electrons, for ethene and mve, or 12 electrons, for butadiene, in every possible way, thus defining the “10 electrons in 8 orbitals” and “12 electrons in 10 orbitals” active spaces, labeled as (10,8) and (12,10), respectively. The electron configuration shown in Scheme 3, and the configuration obtained by moving the two π_g electrons into the rightmost π_g orbital and the other electron to the rightmost one, then the configuration dominating the second $^1\Delta_g$ electronic state of the O_2 molecule. If, on the other hand, the two π_g electrons are split, by assigning one electron to the leftmost π_g orbital and the other electron to the rightmost one, then the configuration dominating the second $^1\Delta_g$ electronic state is obtained. As the alkene and O_2 get closer, other configurations can give a significant contribution, depending on the geometrical approach. Thus, in the various structures to be optimized, two oxygen lone pairs are differently located (the relevant orbitals are depicted in Scheme 4).

In Scheme 4 X designates again hydrogen, methoxy, or vinyl. The additional π , π^* couple of the vinyl group is shown between brackets. For some structures, serious MCSCF convergence problems arised if all oxygen lone pairs were included in the active space. Therefore, two slightly different active spaces were used in the determination of two sets of critical points, as described in the following. The (10,8) and (12,10) active spaces just defined were used to optimize the separated reagents, the dioxetane products, and the transition structures for diradical formation (Scheme 4, left, and Scheme 5, bottom). Then, for the remaining structures, two more restricted active spaces, labeled (8,7) for ethene and mve and (10,9) for butadiene, were defined by excluding the lone-pair orbital sketched in Scheme 4 (top right). This orbital was kept as doubly occupied in all configurations. This was done in order to avoid very lengthy MCSCF iterative processes and inefficient optimization of the remaining structures. The “complete” (10,8) or (12,10) active spaces and the “reduced” (8,7) or (10,9) active spaces cover regions of the energy surfaces which overlap in correspondence of the diradical formation transition structure, as shown in Scheme 5. In fact, this transition structure could be efficiently optimized by following either choice of active space. The two geometries obtained in this case show insignificant changes.

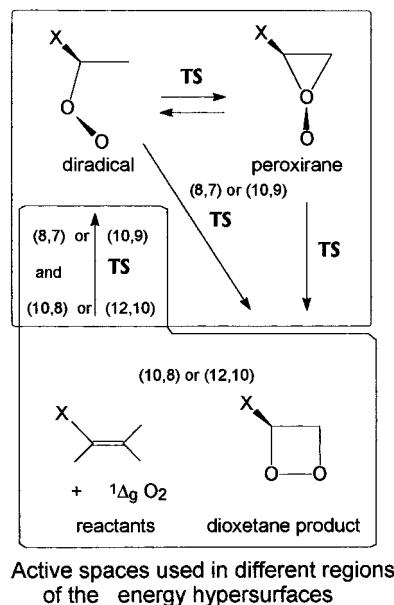
In the final single-point CAS-MCSCF and CAS-PT2 calculations, the excluded lone pairs were reintroduced, together with two more

(39) Roos, B. O.; Andersson, K.; Fülischer, M. P.; Malmqvist, P.-Å.; Serrano-Andres, L.; Pirlloot K.; Mercham, M. *Adv. Chem. Phys.* **1996**, *93*, 219–331.

Scheme 4



Scheme 5



orbitals, additionally included in the active space as “counterparts” of the oxygen lone-pairs orbitals in order to improve convergence (sketched by dashed lines in Scheme 3). Each one of these is similar to the lone-pair orbitals but has out-of-phase contributions on the oxygen atoms involved, whereas the lone-pair orbital has in-phase contributions (Scheme 3, top). This choice defines a “10 electrons in 10 orbitals” final active space, for ethene or mve + O_2 , here noted as (10,10). A (12,12) active space for butadiene + O_2 is similarly defined. These homogeneous energy evaluations, carried out for all structures with the common larger active spaces, yielded the energy differences reported in the tables (total energies are provided in the Supporting Information). The nature of the critical points (energy minima and saddle points of first or higher order) was determined by vibrational analysis.

(B) The stable and transition structures were determined again by gradient procedures⁴⁰ at the DFT(B3LYP)/6-31G(d) level of theory.⁴¹

(40) Pople, J. A.; Gill, P. M. W.; Johnson, B. G. *Chem. Phys. Lett.* **1992**, *199*, 557–560.

Thus the data obtained at three different theory levels can be compared at a uniform basis set level. To get some information on the effects of basis set extension, the energy differences relevant to the three reaction pathways were then recomputed at the DFT(B3LYP)/6-311+G(2d,-2p) level,^{38b} by single-point energy calculations in correspondence of the DFT(B3LYP)/6-31G(d) optimized geometries. Basis set effects were further explored in the butadiene case, by optimizing the peroxirane minimum, the diradical, and the relevant interconversion TS with the 6-311+G(3df,2p) basis set (see next section for details).

The unrestricted DFT calculations on diradical species converge on closed-shell type solutions (zero spin densities). To obtain a qualitatively correct description, two highest occupied/lowest unoccupied orbital rotations are switched on right from the onset, one within the α set and the other within the β set. The resulting description of a diradical species, after the iterative procedure is converged, is qualitatively satisfactory in term of spin densities and is likely to generate reasonable structures. However, this manipulation of the unrestricted wave function induces a strong spin contamination by the triplet in the wave function itself, as evidenced by $\langle S^2 \rangle$ values close to 1. The wave function nature is thus intermediate between singlet and triplet spin multiplicities.^{42a} As a consequence, the energy values obtained by this procedure have to be refined by some spin-projection method, to get rid of the spin contaminants.^{42b} This was done in an approximate way, by eliminating only the largest contaminant, i.e., the triplet, using the formula suggested by Yamaguchi.^{42c}

The DFT and CAS-MCSCF optimizations were carried out using the GAUSSIAN 94 system of programs.⁴³ The natural bond orbital (NBO) analysis,⁴⁴ implemented in that suite, was used to evaluate the natural atomic orbital (NAO) charges. The CAS-MCSCF and CAS-PT2 calculations with the largest active space were done with the MOLCAS 4 program.⁴⁵

Results and Discussion

Concerted Attacks. A preliminary part of this study consisted in checking the critical point geometries corresponding to a

(41) Parr, R. G.; Yang, W. *Density Functional Theory of Atoms and Molecules*; Oxford University Press: New York, 1989; Chapter 3. Becke, A. D. *Phys. Rev. A* **1988**, *38*, 3098–3100. Becke, A. D. *ACS Symp. Ser.* **1989**, No. 394, 165. Becke, A. D. *J. Chem. Phys.* **1993**, *98*, 5648–5652. Lee, C.; Yang, W.; Parr, R. G. *Phys. Rev. B* **1988**, *37*, 785–789.

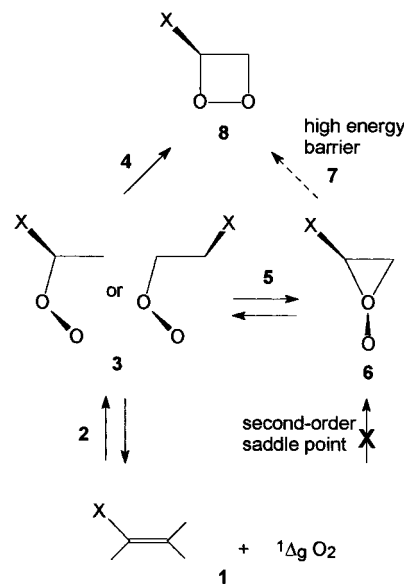
(42) (a) Cramer, C. J.; Dulles, F. J.; Giesen, G. J.; Almlöf, J. *Chem. Phys. Lett.* **1995**, *245*, 165–170. Compare also: Goldstein, E.; Beno, B.; Houk, K. N. *J. Am. Chem. Soc.* **1995**, *118*, 6036–6043. An ancillary observation: the fact that the DFT hypersurface curvature reflects the features of the triplet surface may have some consequences when a bond formation process is considered between “C” and “O” centers in the diradicals, because the repulsive nature of the triplet may introduce an “excess of positive curvature” and raise the barrier. (b) A calculation on ¹O₂ can exemplify the procedure. The original DFT(UB3LYP) calculation would give a singlet–triplet energy gap of 39.3 kcal mol⁻¹. The reference experimental value is 22.5 kcal mol⁻¹. The $\langle S^2 \rangle$ value is zero. Enforcing spin contamination by the orbital mixing procedure provides an $\langle S^2 \rangle$ value of 1.0035, intermediate between the values of a singlet and a triplet multiplicities. The singlet–triplet energy gap is now reduced accordingly to 10.4 kcal mol⁻¹. The projection procedure refines the energy and produces a gap of 20.9 kcal mol⁻¹. (c) Yamanaka, S.; Kawakami, T.; Nagao, K.; Yamaguchi, K. *Chem. Phys. Lett.* **1994**, *231*, 25–33. Yamaguchi, K.; Jensen, F.; Dorigo, A.; Houk, K. N. *Chem. Phys. Lett.* **1988**, *149*, 537–542.

(43) Frisch, M. J.; Trucks, G. W.; Schlegel, H. B.; Gill, P. M. W.; Johnson, B. G.; Robb, M. A.; Cheeseman, J. R.; Keith, T. A.; Petersson, G. A.; Montgomery, J. A.; Raghavachari, K.; Al-Laham, M. A.; Zakrzewski, V. G.; Ortiz, J. W.; Foresman, J. B.; Cioslowski, J.; Stefanov, B. B.; Nanayakkara, A.; Challacombe, M.; Peng, C. Y.; Ayala, P. Y.; Chen, W.; Wong, M. W.; Andres, J. L.; Replogle, E. S.; Gomperts, R.; Martin, R. L.; Fox, D. J.; Binkley, J. S.; Defrees, D. J.; Baker, J.; Stewart, J. P.; Head-Gordon, M.; Gonzalez, C.; Pople, J. A. *GAUSSIAN94*; Gaussian, Inc.: Pittsburgh, PA, 1995.

(44) Reed, A. E.; Weinstock, R. B.; Weinhold, F. *J. Chem. Phys.* **1985**, *83*, 735–746. Reed, A. E.; Weinhold, F. *J. Chem. Phys.* **1983**, *78*, 4066–4073. Foster, J. P.; Weinhold, F. *J. Am. Chem. Soc.* **1980**, *102*, 7211–7218.

(45) Andersson, K.; Blomberg, M. R. A.; Fülscher, M. P.; Karlström, G.; Lindh, R.; Malmqvist, P.-Å.; Neogrády, P.; Olsen, J.; Roos, B. O.; Sadlej, A. J.; Schütz, M.; Seijo, L.; Serrano-Andrés, L.; Siegbahn, P. E. M.; Windmark, P.-O. *MOLCAS Version 4*; University of Lund: Lund, Sweden, **1997**.

Scheme 6



concerted approach. This is easily done for the ethene + dioxygen system (reaction a), and critical points corresponding to supra–supra (ss) and supra–antara (sa) attacks are in fact present on the relevant energy hypersurface (the antara moiety being O₂). However, these critical points have been characterized as higher-order saddle points of no direct chemical importance, in accord with earlier results.^{29,32} Their energy, when compared to that of the separated reagents, is also quite high: 42.0 and 37.0 kcal mol⁻¹, respectively, at the CAS-PT2 level.^{46a} For asymmetrically substituted alkenes (as mve and butadiene) it is clear that the classic distinction between supra–supra and supra–antara approaches becomes evanescent. Actually, for both reactions b and c, a single critical point (of C₁ symmetry) was found for a concerted approach. Its nature was again that of a second-order saddle point.³² The relevant CAS-PT2 energies are 28.0 kcal mol⁻¹, for mve,^{46b} and 33.8, for butadiene.^{46c} The nature of these critical points⁴⁷ makes very unlikely any hypothetical “trajectory” of the system on the energy surface passing through them as. Their high energy works in the same direction.

The remaining (and most important) part of this study is thus focused on attacks taking place through intermediates (diradicals and peroxiranes). These nonconcerted attacks are displayed in Scheme 6, where bold numerals refer to stable species or to

(46) (a) 55.6 and 47.6 kcal mol⁻¹ for ss and sa, respectively, at the CAS-MCSCF level. The DFT(B3LYP)/6-31G(d) estimates are even higher than the CAS-PT2, putting the ss saddle point at 74.4 kcal mol⁻¹ and the sa at 50.8 kcal mol⁻¹. (b) 43.0 kcal mol⁻¹, at the CAS-MCSCF level. (c) 46.5 kcal mol⁻¹, at the CAS-MCSCF level. In the mve and butadiene cases, no DFT computations were carried out.

(47) A supra–supra saddle point is defined for ethene only. It is a third-order saddle point (CAS-MCSCF frequencies: 1756i, 429i, and 56i cm⁻¹). The first Hessian eigenvector is dominated by the distance between the two moieties, coupled with the modification of the CC and OO bond lengths. The second corresponds to an asymmetric opening which points toward a diradical-like deformation. The third one, corresponding to a very flat portion of the energy surface, points toward the supra–antara critical point. The supra–antara critical point found for ethene corresponds to the unique C₁ saddle point detected in the other two cases. All of them are second-order saddle points. One eigenvector (CAS-MCSCF frequency 749i, 453i, and 572i cm⁻¹, for ethene, mve, and *s-trans*-butadiene, respectively) points in the fragmentation direction; its major component is the distance between the midpoint X of the CC bond and the closer oxygen (O¹). The other eigenvector (CAS-MCSCF frequency 663i, 1022i, and 738i cm⁻¹ for ethene, mve, and butadiene, respectively) is directed toward the transition structure for diradical formation, and its principal components are the CXO¹ angle and the OOX¹ dihedral angle.

Table 1. Ethene + $^1\Delta_g$ Dioxygen Reaction Pathway Relative^a Energies

		theory level with basis set			
		CAS-MCSCF ^b 6-31G(d)	CAS-PT2 ^b 6-31G(d)	DFT(B3LYP) ^c	
				6-31G(d)	6-311+G(2d,2p) ^d
ethene + $^1\Delta_g$ O ₂	1a	0.0	0.0	0.0	0.0
diradical formation TS	2a	24.8	17.5	14.4	16.8
diradical minimum	3a	12.1	8.3	6.8	9.7
closure to dioxetane TS	4a	19.9	16.4	15.3	18.5
closure to peroxirane TS	5a	28.2	21.6	21.9	22.9
peroxirane	6a	20.0	18.1	18.9	18.0
peroxirane–dioxetane TS	7a	47.3	43.8	44.8	45.1
dioxetane	8a	−31.1	−31.7	−30.1	−25.5

^a kcal mol^{−1}. ^b (10,10) active space; single-point calculations on the CAS-MCSCF optimized geometries. ^c After the largest spin contaminant has been projected out. ^d Single-point calculations on the DFT(B3LYP)/6-31G(d) optimized geometries.

Table 2. Methyl Vinyl Ether + $^1\Delta_g$ Dioxygen Reaction Pathway Relative^a Energies

		theory level with basis set			
		CAS-MCSCF ^b 6-31G(d)	CAS-PT2 ^b 6-31G(d)	DFT(B3LYP) ^c	
				6-31G(d)	6-311+G(2d,2p) ^d
methyl vinyl ether + $^1\Delta_g$ O ₂	1b	0.0	0.0	0.0	0.0
diradical formation TS	2b	20.7	11.4	9.8	12.0
diradical minimum	3b	6.3	2.3	3.4	6.5
closure to dioxetane TS	4b	14.3	10.9	12.7	15.8
closure to peroxirane TS	5b	20.6	14.6	16.8	18.1
peroxirane	6b	12.6	11.3	13.6	11.3
peroxirane–dioxetane TS	7b	40.4	37.8	41.2	42.0
dioxetane	8b	−39.5	−39.9	−35.7	−30.8

^a kcal mol^{−1}. ^b (10,10) active space; single-point calculations on the CAS-MCSCF optimized geometries. ^c After the largest spin contaminant has been projected out. ^d Single-point calculations on the DFT(B3LYP)/6-31G(d) optimized geometries.

Table 3. *s-trans*-Butadiene + $^1\Delta_g$ Dioxygen Reaction Pathways Relative^a Energies

		theory level with basis set			
		CAS-MCSCF ^b 6-31G(d)	CAS-PT2 ^b 6-31G(d)	DFT(B3LYP) ^c	
				6-31G(d)	6-311+G(2d,2p) ^d
<i>s-trans</i> -butadiene + $^1\Delta_g$ O ₂	1c	0.0	0.0	0.0	0.0
diradical formation TS	2c	20.9	11.7	8.8	10.8
diradical minimum	3c	3.8	−2.8	−3.9	−1.1
closure to dioxetane TS	4c	15.1	8.8	7.2	10.5
closure to peroxirane TS ^e	5c	25.2	18.0		
peroxirane ^e	6c	20.7	19.5		
peroxirane–dioxetane TS	7c	44.6	41.4	42.5	40.6
dioxetane	8c	−26.7	−26.8	−26.6	−22.7

^a kcal mol^{−1}. ^b (12,12) active space; single-point calculations on the CAS-MCSCF optimized geometries. ^c After the largest spin contaminant has been projected out. ^d Single-point calculations on the DFT(B3LYP)/6-31G(d) optimized geometries. ^e Missing values: the relevant geometries were optimized with a larger basis set (see text).

transition structures and X = H, OMe, and vinyl.

The energy differences of the critical points relative to the separated reagents **1** are collected in Tables 1–3 for reactions a–c, respectively. Total energies are provided in the Supporting Information. The overall energy profiles for the transformations examined are displayed in Figures 4–6, again for reactions a–c, respectively. Bold numerals are used again in both tables and energy profiles to mark consistently the critical points. Thus, in order from the left to the right in Figures 4–6, the diradical formation pathway is recognizable as marked by the numerals **1–2–3**. Similarly, the diradical ring closure to dioxetane is marked as **3–4–8**, the diradical ring closure to peroxirane as **3–5–6**, and, finally, the peroxirane transformation to dioxetane as **6–7–8**. Only the three more interesting transition structures for the mve and *s-trans*-butadiene reactions are shown in Figures 1–3 (the reported interatomic distances are in angstroms and angles in degrees). These correspond to entries **4a,b**, **5a,b**, and **7a,b** of the tables, respectively.

Diradical Pathway to Dioxetane. Diradical intermediates are found to be present in all three reactions, along nonconcerted

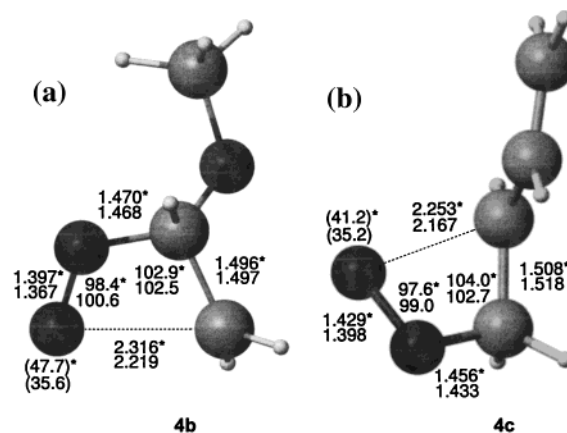


Figure 1. Transition structures **4b** (a) and **4c** (b), relevant to the ring closure of the diradicals to dioxetanes, for reactions b and c, which involve mve and *s-trans*-butadiene, respectively. Key: CAS-MCSCF/6-31G(d) (starred values); DFT(B3LYP)/6-31G(d) (plain values). Interatomic distances are in angstroms, and angles, in degrees (dihedral angles in parentheses).

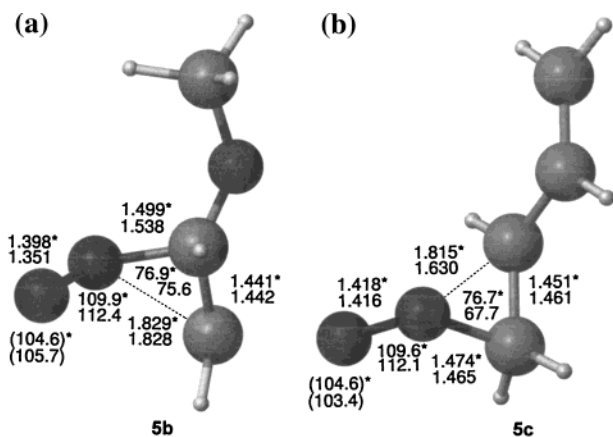


Figure 2. Transition structures **5b** (a) and **5c** (b), relevant to the ring closure of the peroxy diradicals to peroxirane structures, for reactions b and c, which involve mve and *s-trans*-butadiene, respectively. Key: CAS-MCSCF/6-31G(d) (starred values); DFT(B3LYP)/6-31G(d) for (a), DFT(B3LYP)/6-311+G(3df,2p) for (b) (plain values; see text). Interatomic distances are in angstroms, and angles in degrees (dihedral angles in parentheses).

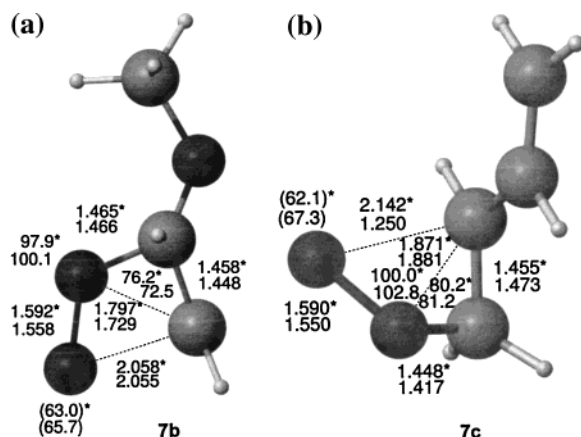
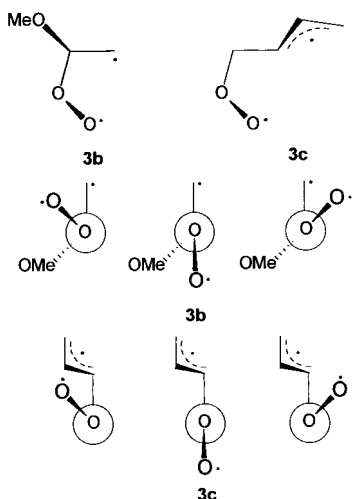


Figure 3. Transition structures **7b** (a) and **7c** (b), for methoxy peroxirane and vinyl peroxirane transformation to the related dioxetanes. Key: CAS-MCSCF/6-31G(d) (starred values); DFT(B3LYP)/6-31G(d) (plain values). Interatomic distances are in angstroms, and angles in degrees (dihedral angles in parentheses).

Scheme 7



pathways connecting the reagents to the dioxetane products. In the substituted systems, O₂ attacks on different sp² carbons correspond to different diradical intermediates. Moreover, three

different conformations exist, for a total of six energy minima. For mve, the attack on the methoxy-substituted carbon gives origin to the more stable intermediate (CAS-MCSCF results). This had already been observed in several instances and commented by Harding and Goddard.²⁶ In the case of butadiene, dioxygen prefers to attack one terminal CH₂ instead of a central CH, because it creates a delocalized allylic system. The terminal oxygen, in one conformational minimum of each diradical, is anti with respect to the other carbon involved in the [π2 + π2] cycloaddition. Thus, it cannot close directly, while the other two gauche minima can give ring closure (Scheme 7; the labels **3b,c** make reference to the same diradical structures displayed in the Figures 5 and 6). Only one of the two similar gauche pathways (which come about as being the easiest from preliminary explorations) is discussed in the following.

Diradical formation from separate reagents **1** requires the overcoming of the energy barriers relevant to the transition structures **2**. The assessment of the energy barriers shows some dependence on the method used (Tables 1–3). The CAS-PT2 and DFT(B3LYP) estimates are in reasonable accord, differing by 3.1 kcal mol⁻¹ for ethene, 1.6 kcal mol⁻¹ for mve, and 2.9 kcal mol⁻¹ for butadiene (with the same basis set, 6-31G(d)). All diradicals **3** are kinetically stable with respect to back-dissociation, presenting energy barriers whose height is comparable to that for closure to the 4-term ring product (see below). Their CAS-PT2 and DFT estimates are again not too divergent: 9.2 and 7.6 kcal mol⁻¹, respectively, for ethene (Table 1); 9.1 and 6.4 kcal mol⁻¹ for mve (Table 2); 14.5 and 12.7 kcal mol⁻¹ for butadiene (Table 3). Dioxetanes **8** can form from the diradicals **3** if barriers of 8–9 kcal mol⁻¹, for ethene and mve, or ca. 11 kcal mol⁻¹, for butadiene, are surmounted. All reactions are quite exoergic, in the order |ΔE|(mve) > |ΔE|(ethene) > |ΔE|(butadiene). Figure 1 displays the transition structures **4b,c** for ring closure to dioxetanes of the O₂ diradical adducts to mve and *s-trans*-butadiene.

Peroxisane Formation Pathway. At the CAS-MCSCF level, a perepoxydic intermediate **6** is present on the three reaction hypersurfaces as a minimum (Tables 1–3). Thus, peroxirane is described as kinetically stable with respect to fragmentation to reagents, conversion to the diradical, or transformation to dioxetane. However, its direct formation from the alkene and singlet oxygen is not possible, because the corresponding peroxirane-like saddle point endowed with C_s symmetry in the ethene case, results to be a second-order saddle point, and not a transition structure. In fact, this structure has two imaginary vibrational frequencies, which correspond to eigenvectors of the analytic Hessian related to negative eigenvalues.⁴⁸ Thus, this structure is not of direct chemical interest. At the CAS-MCSCF/CAS-PT2 level, the peroxirane minimum can be attained by passing through the diradical intermediate **3** in all three systems. The CAS-PT2 energies of the peroxirane-like second-order saddle points relative to the separated reactants are the following: 26.0 kcal mol⁻¹, for ethene,^{49a} 17.3 kcal mol⁻¹, for mve,^{49b} 24.0 kcal mol⁻¹, for butadiene.^{49c} The transition structures for diradical formation for these three systems are located lower in

(48) In the peroxirane-like second-order saddle points, the first eigenvector (CAS-MCSCF frequency 1721i, 627i, and 1628i cm⁻¹, for ethene, mve, and *s-trans*-butadiene, respectively) is dominated by the distance between the midpoint X of the CC bond and the closer oxygen (O¹), coupled with the OO bond length. The second eigenvector (CAS-MCSCF frequency 483i, 388i, and 417i cm⁻¹ for ethene, mve, and butadiene, respectively) is approximately directed toward the transition structure for diradical formation, and its principal component is the CXO¹ angle.

(49) (a) 36.3 kcal mol⁻¹, at the CAS-MCSCF level. (b) 28.2 kcal mol⁻¹, at the CAS-MCSCF level. (c) 34.8 kcal mol⁻¹, at the CAS-MCSCF level.

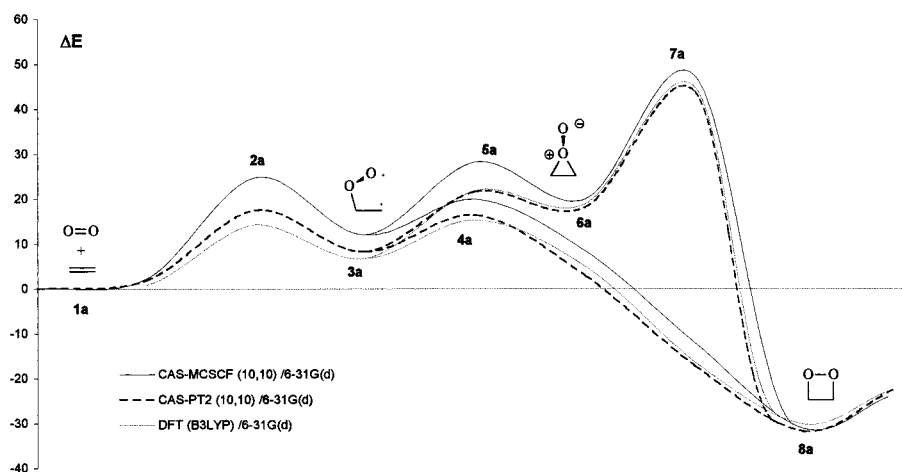


Figure 4. Energy profiles for reaction a (singlet dioxygen + ethene). Energy differences are in kcal mol⁻¹. Key: CAS-MCSCF, solid line; CAS-PT2, bold dashed line; DFT, dashed line.

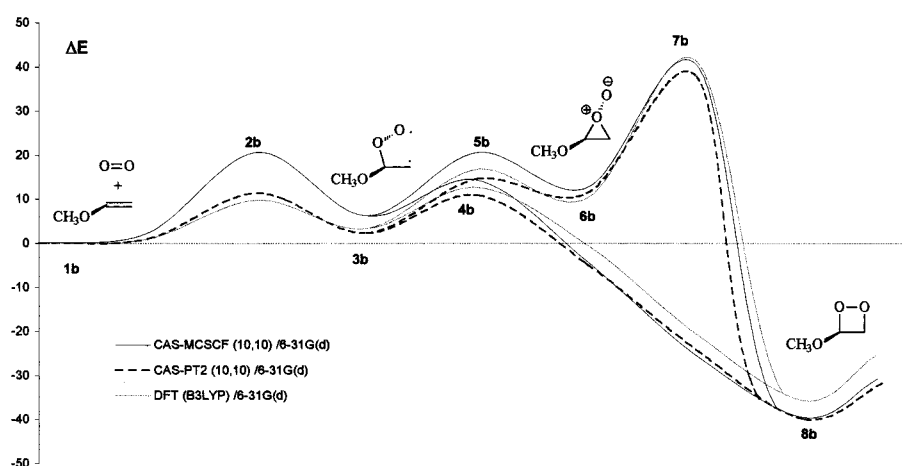


Figure 5. Energy profiles for reaction b (singlet dioxygen + mve). Energy differences are in kcal mol⁻¹. Key: CAS-MCSCF, solid line; CAS-PT2, bold dashed line; DFT, dashed line.

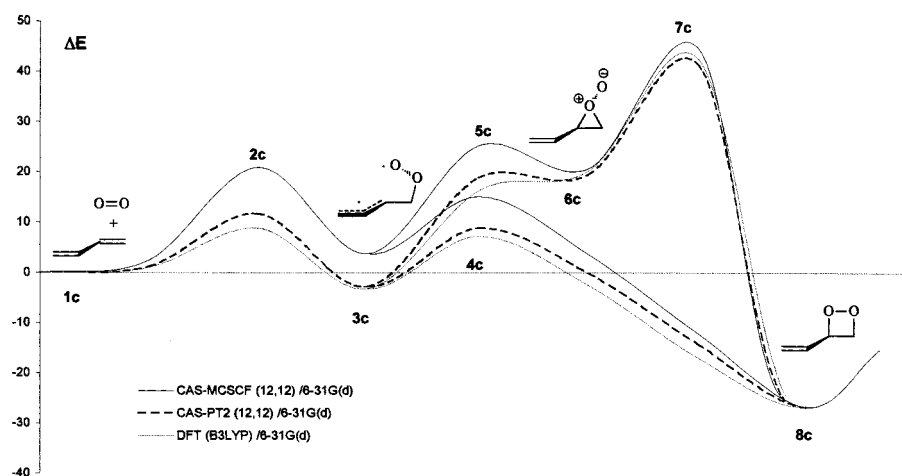


Figure 6. Energy profiles for reaction c (singlet dioxygen + butadiene). Energy differences are in kcal mol⁻¹. Key: CAS-MCSCF, solid line; CAS-PT2, bold dashed line; DFT, dashed line.

energy than the peroxirane-like second-order saddle points by 8.5, 5.9, and 12.3 kcal mol⁻¹, for ethene, mve, and butadiene, respectively (Tables 1–3).

Figure 2 shows the transition structures **5b,c** for ring closure of the peroxy diradicals to the relevant peroxiranes.

Energy barriers for diradical closure to peroxirane of 13–15 kcal mol⁻¹, in the ethene case, and 12–13 kcal mol⁻¹, for mve, are estimated by the CAS-PT2 and DFT methods, which appear

to be in accord. A diradical-to-peroxirane “barrier” of ca. 21 kcal mol⁻¹ for *s-trans*-butadiene is estimated through the single-point CAS-PT2 calculations, but the corresponding “peroxirane” single-point calculation gives an energy which is above that for the diradical/peroxirane interconversion TS by 1 kcal mol⁻¹. Moreover, the peroxirane formation barriers from the diradical are only 4–6 kcal mol⁻¹ higher than that for diradical closure to dioxetane in the first two cases, but the “barrier” estimate

for *s-trans*-butadiene is ca. 10 kcal mol⁻¹ higher. On the whole, this pathway seems to be viable only in the first two cases.

At the DFT level, in the *s-trans*-butadiene case, no clear peroxirane energy minimum is found. In correspondence of a peroxirane-like geometry, only a *shoulder zone* appears to be present on the energy surface (i.e. a flat portion of the energy surface, with very low gradient, and contrasting curvatures at its periphery). In fact, the corresponding structure is unstable toward ring-opening, and this leads to the diradical. Basis set effects were explored in this case, by attempting to optimize the peroxirane minimum and the relevant ring-opening TS with the 6-311+G(3df,2p) basis set (to set an energy reference, also the diradical was reoptimized). It was thus possible to determine the structures of both critical points (the TS optimum parameters are reported in Figure 2b). Vinyl peroxirane corresponds at this point to an energy minimum located 19.9 kcal mol⁻¹ above the diradical intermediate. However, basis set extension has a very modest effect, and the tiny energy barrier for peroxirane ring opening is only 0.02 kcal mol⁻¹ high. In conclusion, a vinyl peroxirane structure can be considered unstable.

The C–O bond cleavage involved in the peroxirane to diradical transformation is triggered by a stereoelectronic effect, in that the vinyl substituent rotates in order to give conjugation with the p_C orbital involved in the σ_{CO} bond, and conjugation generates a delocalized allyl radical π-system. With regard to this aspect, in the case of *s-trans*-butadiene, peroxirane opens rather easily to the diradical also at the CAS-MCSCF level ($\Delta E^\ddagger = 4.5$ kcal mol⁻¹, Table 3). By contrast, the other two peroxirane to diradical back-transformation barriers are ca. 8 kcal mol⁻¹ (Tables 1 and 2). All values are lowered to some extent at the CAS-PT2 level (to 3.3 kcal mol⁻¹, for ethene, and 3.5 kcal mol⁻¹, for mve). Similarly low estimates for the back-transformation to a diradical are obtained at the DFT theory level, using the same basis set (2.0 kcal mol⁻¹, for ethene, and 3.2 kcal mol⁻¹, for mve). However the single-point energy evaluation with the more extended basis set raise again the estimate to some extent to 4.0 and 6.8 kcal mol⁻¹. On one hand, this effect is apparently sufficient (but only at the DFT level) to impede peroxirane formation in the case of *s-trans*-butadiene. On the other hand, the CAS-PT2 data (in correspondence of the CAS-MCSCF geometries) locate the vinyl-substituted peroxirane at higher energy than the TS for its interconversion with the diradical (Table 3). This suggests that dynamical correlation effects can contribute to the vinyl-substituted three-membered ring instability.⁵⁰

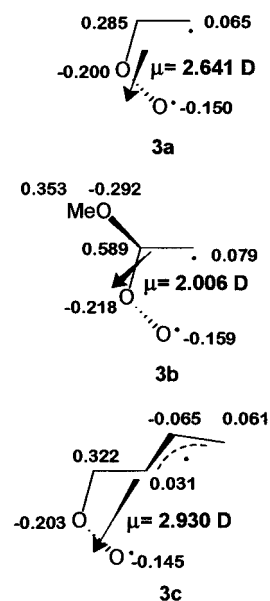
Peroxirane to Dioxetane Conversion. This step, although taking place through a first-order saddle point **7**, requires the overcoming of a high energy barrier and is not competitive with the back-transformation of peroxirane to diradical. The barrier heights are 26–27 (ethene), 27–31 (mve), or 22–24 kcal mol⁻¹ (*s-trans*-butadiene). In this last case, the peroxirane to dioxetane rearrangement TS determined at the DFT(B3LYP)/6-31G(d) level connects a minimum (dioxetane) to a shoulder zone.

The two transition structures **7b,c** for methoxy and vinyl peroxirane transformation to the related dioxetanes are shown in Figure 3.

A few comments can be added on how the present theoretical results compare with the experimental studies carried out on

(50) Carrying out single-point higher-level calculation on geometries optimized at a lower theory level is common practice. This action obviously results in probing the higher-level energy hypersurface with some approximation. In other words, the TS location along the reaction pathway on one surface, and the reaction pathway itself, could be shifted to some extent with respect to their counterparts on the other surface. Thus, in the CAS-PT2 energy difference estimations, a “geometrical factor” is intermingled with dynamical correlation effects.

Scheme 8



similar systems. In some of them the hypothesis of open-chain zwitterionic (diradical) intermediates appeared to explain the results collected.^{23a-d} Those investigations were dealing with $[\pi 2 + \pi 2]$ singlet oxygen cycloadditions on 1,4-dialkoxybutadienes or 2,4-hexadienes. In other studies, some of which dealing with enol ethers,^{12b,15c,18b} the peroxirane hypothesis, or that of an exciplex, were more persuasive. The intervention of a peroxirane intermediate has also been inferred in a recent study of the ene and $[\pi 2 + \pi 2]$ competition on 2,5-dimethyl-2,4-hexadiene.^{9b} Many investigations deal with systems open to the ene reaction. It is conceivable that, starting from a peroxirane intermediate, the ene pathway could be rather easy, in contrast with the result just discussed for the peroxirane to dioxetane pathway. However, in view of the present results, when both the ene and $[\pi 2 + \pi 2]$ reaction pathways are viable, the possible presence of a bifurcation in correspondence of an open-chain zwitterionic intermediate has to be considered. This zwitterion could be the common intermediate to the ene and $[\pi 2 + \pi 2]$ reactions and not peroxirane. The solvent polarity could then determine which reaction pathway is preferred, either closing the open-chain zwitterion to dioxetane or converting it to peroxirane followed by an ene TS. It is experimentally known that a higher polarity favors the $[\pi 2 + \pi 2]$ reaction. However, the present theoretical study does not include solvation effects. Up to this point, we can only observe that the three peroxy diradicals are already endowed with a significant polarity (zwitterionic character), as described by their dipole moments and NAO⁴⁴ charges (Scheme 8). They can thus be considered as legitimate representatives of pathways proceeding via open-chain intermediates of “not strictly diradical” nature.

Conclusions

Although the set of CH₂=CHX substrates considered in the present study is limited to the three cases X = H, OCH₃, and CH=CH₂, the same qualitative description of the $[\pi 2 + \pi 2]$ reaction mechanism has been obtained in all cases. Peroxirane, which is attainable only by passing through the diradical, is defined as a neat energy minimum on the energy hypersurface only in the first two cases. For ethene and methyl vinyl ether the energy barrier for the ring closure of the relevant diradical to a peroxirane intermediate is higher than that for the diradical

closure to dioxetane by 4–6 kcal mol⁻¹. For butadiene the energy difference between the two barriers is estimated 10 kcal mol⁻¹. However, the results obtained in this study on the [$\pi 2 + \pi 2$] reaction indicate that, although a peroxirane intermediate might form in some cases, this is a dead-end pathway, unable to lead to dioxetane. This is due to the high energy barriers (larger than 22 kcal mol⁻¹) found for the second step, the rearrangement of peroxirane to dioxetane. Opposed to this

substantial barrier is the rather easy backward step from peroxirane to the diradical.

Acknowledgment. Financial support has been provided by the Italian MURST and by the Italian CNR (within the Progetto Strategico “Modellistica Computazionale di Sistemi Molecolari Complessi”). The figures were drawn with MolMol 2.4.⁵¹

Supporting Information Available: Tables of computational energies. This material is available free of charge via the Internet at <http://pubs.acs.org>.

(51) MolMol 2.4. A graphic program developed by the Institut für Molekular-biologie und Biophysik, EHT Zurich Spectrospin AG, Faellenden, Switzerland: Koradi, R.; Billeter, M.; Wütrich, K. *J. Mol. Graphics* **1996**, *14*, 51–55.

JA990805A